

TOWARDS HIGHER EFFICIENCIES FOR CRYSTALLINE SILICON SOLAR CELLS USING SiC LAYERSStefanie Riegel¹, Bernd Raabe¹, Roman Petres¹, Sangeeta Dixit³, Lisong Zhou³, Giso Hahn^{1,4}¹ University of Konstanz, Department of Physics, Jacob-Burckhardt-Str. 29, 78457 Konstanz, Germany³ Applied Materials, 3050 Bowers Avenue, Santa Clara, CA 95054-3299, USA⁴ also with Fraunhofer Institute for Solar Energy Systems (ISE), Heidenhofstr. 2, 79110 Freiburg, GermanyEmail: Stefanie.Riegel@uni-konstanz.de, Tel: +49 7531 88 2074, Fax: +49 7531 88 3895

ABSTRACT: We investigate the surface passivation potential of SiC on symmetrical lifetime samples and on cell level. To investigate the influence of the deposition conditions on the passivation quality, lifetime measurements on symmetrical samples using the QSSPC technique were performed. The symmetrical lifetime samples were fired to simulate the 'fire through' process used in a standard screen printed solar cell process. Maximum effective lifetime measured on n-type substrate was 3.7 ms at CH₄/SiH₄=1. Firing of the samples led to a drop in effective lifetimes of about one decade. Maximum effective lifetime after firing was 148 μs at CH₄/SiH₄=6. To avoid losses in passivation quality caused by the firing step, a buried contact solar cell process was chosen. As cell metallization is done via electroless plating in this process, no firing step is necessary. Rear contacts were realized by laser fired contacts. Reference cells were processed with full area Al-BSF. Fillfactors were reduced because of front side metallization problems. IQE in the long wavelength regime is significantly higher for the SiC passivated cell than for the cell with Al-BSF. Fitting of the IQE data gave rear a SRV of 520-600 cm/s for the cell with SiC passivation and 750-900 cm/s for the cell with Al-BSF.

Keywords: Silicon Carbide, Passivation, Buried Contact Solar Cell

1 INTRODUCTION

The need for cost reduction in solar cell fabrication necessitates thinner wafers and higher cell efficiencies. Therefore, rear surface passivation becomes more and more important [1]. Silicon carbide (SiC) layers have already shown excellent surface passivation properties [2,3] on n- and p-type material.

In this paper we explored the dependency of surface passivation qualities of SiC layers on deposition parameters and the firing stability of these layers. The layers with the best passivation quality were applied to buried contact solar cells of 125x125 mm² cell area. Layers were fabricated by plasma enhanced chemical vapor deposition (PECVD) using different ratios of the process gases CH₄/SiH₄ and different values for radio frequency power. As surface treatment before deposition heavily influences the passivation quality [4] wafers were cleaned in an H₂O₂ + H₂SO₄ mixture and received a HF dip directly before deposition. A HF dip with subsequent short in-situ plasma etching step [5] are reported for pretreatment as well.

To investigate the passivation properties of SiC layers on cell level buried contact solar cells with selective emitter and silicon carbide passivation were processed. Due to the fact that metallization is done via electroless plating of nickel and copper no firing step is applied in the process. This allows to make use of the excellent passivation qualities of SiC. Reference cells were fabricated with Al-BSF. Solar cell properties were investigated by taking the IV- and spectral response (SR) data as well as by light beam induced current measurements (LBIC).

2 LIFETIME MEASUREMENTS**2.1 Sample preparation**

For sample preparation <100> oriented n- and p-type FZ wafers were used. Wafer resistivity was 1.5 Ωcm for n-type and 2.5 Ωcm for p-type material. Wafer thickness was 260 to 280 μm (n-type) respectively 275 to 325 μm (p-type).

Samples were cleaned at University of Konstanz (UKN) using hot (80°C) H₂O₂ + H₂SO₄ (1:4). The Piranha-oxide remained on the wafers during transfer to Applied Materials for surface protection. Directly before introducing the wafers into the PECVD reactor the wafers were etched in HF (5%) to remove the oxide and guarantee for a clean surface.

2.2 SiC layer deposition

Silicon carbide layers of about 100 nm thickness were deposited on both sides of the wafers at Applied Materials by PECVD. Depositions were carried out with different methane to silane ratios and different values for radio frequency power. Methane to silane ratios used ranged from one to twelve. Lifetime measurements were carried out before and after firing using the Quasi Steady State Photoconductance technique (QSSPC) [6]. The samples were fired under conditions that correspond to the ones solar cells undergo in a standard Al-BSF formation step. Firing was carried out in an industrial type belt furnace with a peak temperature of about 800°C for 2 s.

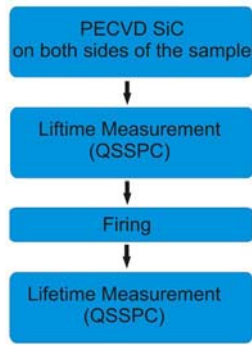


Figure 1: Preparation of the symmetrical samples for lifetime measurements. For SiC deposition an Applied Materials platform was used. Sample firing was performed under standard conditions ($T_{\text{peak}} \sim 800^{\circ}\text{C}$, 2 s) in an industrial type belt furnace.

2.3 Results

Effective lifetimes were measured at an injection level of 10^{15} cm^{-3} using the QSSPC technique. Figure 2 shows the effective lifetime measured on the n-type samples deposited at two different values for the radio frequency power. Maximum effective lifetimes of 3.7 ms were reached at $\text{CH}_4/\text{SiH}_4=1$. Effective lifetimes decrease with increasing CH_4/SiH_4 . After the firing step effective lifetimes are significantly lower than before and the dependency on the gas ratio changes. The maximum effective lifetime measured after firing drops to $148 \mu\text{s}$. Maximum effective lifetimes after firing are reached at a methane to silane ratio of six for both values of radio frequency power. There is no significant effect of radio frequency power on effective lifetimes.

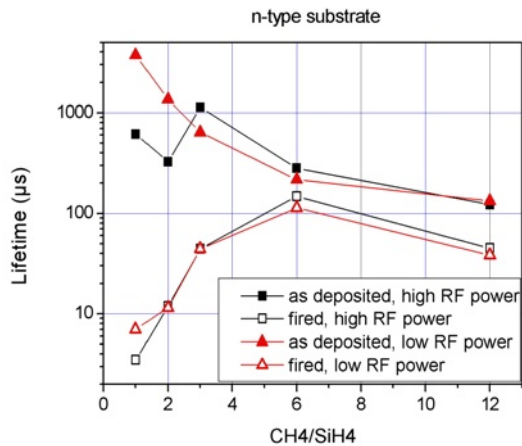


Figure 2: Effective lifetimes measured on n-type wafers passivated by silicon carbide layers at varying deposition conditions. Maximum effective lifetimes of 3.7 ms are reached. Effective lifetimes drop to $\tau_{\text{max}} = 148 \mu\text{s}$ after firing.

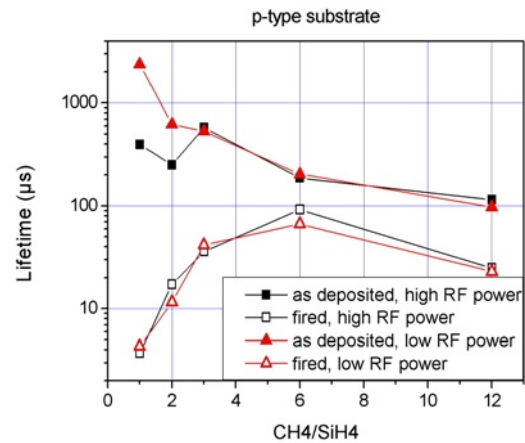


Figure 3: Effective lifetimes measured on p-type wafers passivated by silicon carbide layers at varying deposition conditions. Effective lifetimes on p-type wafers show the same characteristics as on n-type material.

Effective lifetimes for p-type wafers passivated with silicon carbide show the same characteristics as the ones on n-type material. Like on n-type material maximum effective lifetimes after firing are reached at a methane to silane ratio of six. Absolute values of the effective lifetime are lower on p-type samples (see figure 3).

3 SOLAR CELL PROCESSING

3.1 Cell process

To make use of the good SiC passivation possibilities in a solar cell process, the buried contact solar cell concept was chosen. This cell concept has the advantage that no firing as in a standard screen printed cell is necessary, since metallization is done by electroless deposition of nickel and copper. Buried contact solar cells have a high efficiency selective emitter scheme on the front side. Silicon carbide deposited with $\text{CH}_4/\text{SiH}_4=1$ and low radio frequency power was used for rear side passivation. Reference cells with full aluminium back surface field were also processed (see figure 4). The cells were fabricated on $125 \times 125 \text{ mm}^2$ p-type Cz wafers of $240 \mu\text{m}$ thickness. The aluminium back surface field was fabricated by screen printing and firing. Excessive aluminium was removed by etching in HCl and a $2 \mu\text{m}$ thick Al layer was evaporated as an aid for plating. The contacts were formed by electroless nickel/copper plating. Solar cells with silicon carbide passivation were processed with evaporated aluminium on the rear side. Local contact formation on the rear side was realized by local laser contact firing (LFC, see figure 5). As this was a first test of the concept, a very small batch of only two wafers per group was processed.

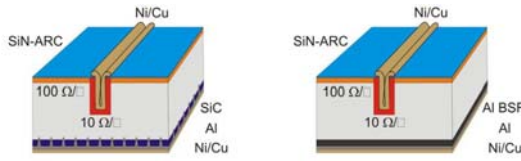


Figure 4: Buried contact solar cells. Rear side passivation of the cell shown on the left side is done using SiC. The rear contact is formed via LFC. The cell on the right side has a full area Al-BSF.

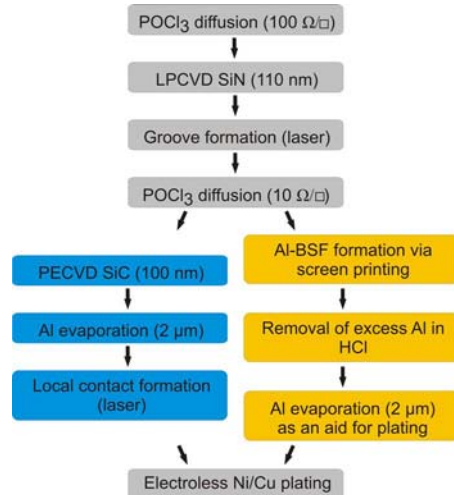


Figure 5: Buried contact process sequence. On the left the process sequence for the SiC passivated cell is shown, on the right the reference process with a full area Al-BSF.

3.2 IV-Measurements

IV-measurements were performed under one-sun illumination. Temperature was controlled to 25°C. The IV-results of the best cells are shown in table I. The buried contact cell with the silicon carbide passivation shows a 5 mV increase in V_{OC} and a 0.3% absolute higher efficiency. Efficiencies are limited due to reduced fillfactors. The low fillfactors on all cells are due to problems in metallization resulting in a rather low finger conductivity of about 0.8 Ω/cm (measured after separating fingers with a dicing saw). An additional loss in fillfactor may be caused by the omitted nickel sintering, that is usually used to form a low ohmic and mechanically stable contact. The SiC passivated cell shows a 0.8% absolute lower fillfactor compared to the full area Al-BSF cell. The laser fired contact scheme was not fully optimized in regard to pitch distance, contact diameter and used laser parameters due to the small amount of samples. We expect higher fillfactors with optimized contacts on the front and rear side.

Table I: IV-results of the best cells.

	FF [%]	j_{SC} [mA/cm ²]	V_{OC} [mV]	H [%]
SiC	74.8	36.0	626.4	16.9
Al-BSF	75.6	35.4	620.8	16.6

3.3 Quantum efficiency

The measurement of the internal quantum efficiency (IQE) of the SiC cell is shown in figure 7. A spot of 2x2 cm² was measured in the middle of the solar cells (see figure 8). IQEs above 70% at 1100 nm were reached. This increase in the IQE is caused by an improved surface passivation of the rear side and good optical properties, that means high internal rear side reflection.

To extract the effective rear Surface Recombination Velocity (SRV) the measured IQE curves were fitted to an IQE evaluation model. A computer program written by B. Fischer [7] based on the model of R. Brendel [8] was used.

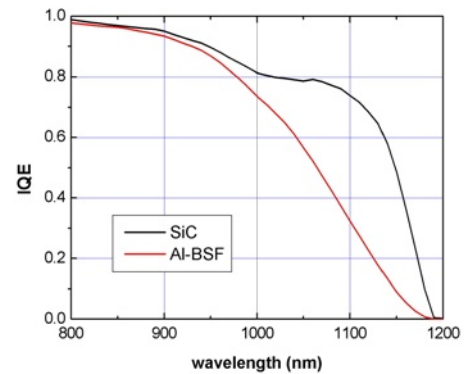


Figure 6: Long wavelength IQE of a buried contact solar cell with silicon carbide passivation in comparison to a buried contact solar cell with Al-BSF.

The optical parameters were obtained via fitting the measured reflectance. For the SiC cell an internal rear side reflectance of 99.6% and a Lambert factor $\Gamma=0$ was found. For the texture angle α we set $\cos(\alpha)=0.9$ (random pyramid texture). Modelling the IQE with these optical values gave an effective rear SRV in the range of 520 to 600 cm/s. For the Al-BSF cell 83.4% rear side reflection and $\Gamma=0.72$ were found resulting in an effective rear SRV between 750 and 900 cm/s. The optical parameters of our Al-BSF structure are better than usually obtained via screen printing. This is due to the removal of the excessive aluminium followed by Al evaporation (see process sequence in figure 5). Normally, rear side reflectance achieved by screen printing is in the range of 60-70%.

The LBIC map shown in figure 8 belongs to the best SiC passivated cell. It is measured at a wavelength of 910 nm. Passivation quality is best in the centre of the cell. Inhomogeneities on the upper and lower edge of the cell are probably caused by wafer handling. The inhomogeneities named A appear to be imprints of tweezers, the ones marked B are due to scratches. As passivation via dielectric layers is very sensitive to surface conditions proper wafer handling is essential.

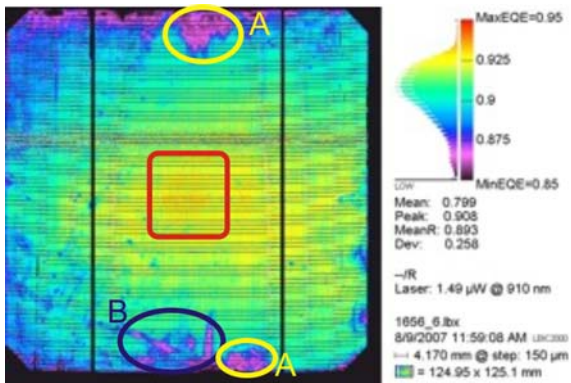


Figure 7: LBIC mapping of a buried contact solar cell with silicon carbide passivation. The spectral response of the cell (see figure 7) was measured over the red square. The regions named A appear to be imprints of tweezers, the ones marked B are due to scratches.

4 CONCLUSIONS

We showed that silicon carbide layers allow for an extremely good surface passivation. Effective lifetimes up to 3.7 ms were reached on n-type material at $\text{CH}_4/\text{SiH}_4=1$. Lifetimes decreased with increasing CH_4/SiH_4 . After firing effective lifetimes were reduced to a maximum lifetime of 148 μs . The maximum effective lifetime was reached at a CH_4/SiH_4 ratio of 6. Using SiC in solar cell fabrication we obtained 5 mV higher open circuit voltages than using an Al-BSF. The effective rear SRV of the SiC cell is almost a factor two lower than the one of the Al-BSF cell (520-600 cm/s versus 750-900 cm/s). This is due to better passivation qualities of the SiC layer and improved optical qualities of the SiC and evaporated aluminium stack system. The LBIC mapping shows that the cells have a high potential for further enhancement in cell efficiency.

5 REFERENCES

- [1] A.G. Aberle, Surface passivation of crystalline silicon solar cells: a review, *Progress in Photovoltaics: Research and Application* 8 (2000) 473.
- [2] I. Martín et al., Surface passivation of n-type crystalline Si by plasma-enhanced-chemical-vapor-deposited amorphous $\text{SiC}_x\text{:H}$ and amorphous $\text{SiC}_x\text{N}_y\text{:H}$ films, *Appl. Phys. Lett.* 81 (2002) 4461.
- [3] S. Janz et al., Phosphorus-doped SiC as an excellent p-type Si surface passivation layer, *Appl. Phys. Lett.* 88 (2006) 133516.
- [4] H. Angermann et al., Wet chemical passivation and characterisation of silicon interfaces for solar cell applications, *Sol. En. Mat. and Sol. Cells* 83 (2004) 331.
- [5] S. Janz et al., Passivation mechanisms of amorphous $\text{Si}_x\text{C}_{1-x}$ layers on highly doped and textured Si surfaces, *Proc. 22nd EU PVSEC, Milan 2007*, 1454.
- [6] R.A. Sinton et al., Contactless determination of current-voltage characteristics and minority carrier lifetimes in semiconductors from quasi-steady-state photoconductance data, *Appl. Phys. Lett.* 69 (1996) 2510.
- [7] B. Fischer, Loss analysis of crystalline silicon solar cells using photoconductance and quantum efficiency measurements, PhD thesis (2003) University of Konstanz.
- [8] R. Brendel et al., Effective diffusion length for minority carriers in solar cells as determined from internal quantum efficiency analysis, *J. Appl. Phys.* 85 (1999) 3634.